

DEVELOPMENT OF A HIGH BRIGHTNESS ELECTRON GUN FOR THE ACCELERATOR TEST FACILITY AT BROOKHAVEN NATIONAL LABORATORY\*

CONF-880695--67

K. Batchelor, H. Kirk, J. Sheehan and M. Woodle  
 Brookhaven National Laboratory,  
 Upton, New York 11973  
 and  
 K. McDonald  
 Princeton University

BNL--41767

DE89 002179

1988

Abstract

An electron gun utilizing a radio frequency accelerating cavity operating at a frequency of 2856MHz is described. Low level tests of a model cavity designed for use with either a thermionic or laser driven photo-cathode are presented. Calculations for a laser driven photo-cathode at a bunch charge of 1nC in a 5psec bunch are given. With this configuration we hope to achieve an emittance ( $\gamma\sigma_x\sigma_x$ ) of 5 to  $10 \times 10^{-6}$  m.rad at an output energy of 4.85 MeV for a 1nC charge.

Introduction

The Brookhaven Accelerator Test Facility is a 50-100MeV electron linac designed to produce electron bunches which can be synchronized with the 5p sec pulse of a 100G Watt CO<sub>2</sub> laser. This facility will be used to study the acceleration of electrons by the laser grating technique,<sup>1</sup> for inverse free electron laser studies<sup>2</sup> and to provide a picosecond source of x-rays via non-linear compton scattering.<sup>3</sup> Figure 1 is a block diagram of the linac and laser components as described in Reference (4). Here we report on the design of the electron gun which will provide r.f. bunches of up to  $10^{10}$  electrons synchronized with the laser beam.

\* Optimum design of the r.f. cavity minimizes emittance growth due to non-linear components of the transverse electric and magnetic fields.

For the ATF gun design we maximize the beam brightness by use of the highest possible accelerating field at the photo-cathode and the shortest laser pulse. The design parameters are summarized in Table I and a section through the gun is shown in Figure 2.

Table I. RF Gun Design Parameters

Structure type.	Resonant
Structure inner diameter, mm	83.08
Structure length, mm	78.75
Number of cells	1+1/2
Operating frequency, GHz	2.856
Beam Energy, MeV	4.85
Beam aperture, mm	20
Shunt Impedance, MΩ/m	57
Cavity Q	11,800
Max. Surface Electric Field, MV/m	118
Average accelerating gradient, MV/m	66.6
Electric field on cathode, MV/m	100
Cavity Stored Energy, J	3.5
Cavity Peak Power, MW	5.3

Design Considerations

The ideal gun design would preserve the emittance of the electron beam as it emerges from the cathode. In practice two effects blow up this initial emittance. Electromagnetic interactions among the electrons (space charge effect), lead to a real increase in phase space volume, while non-linear radial dependence of the transverse components of the external electromagnetic fields lead to an apparent growth of phase volume which cannot be later corrected with linear beam optics.

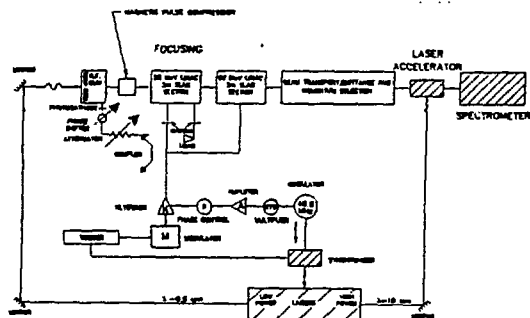


Figure 1. Schematic Diagram of Accelerator Test Facility

The gun is based on the design of Frazer et al<sup>5</sup> who incorporated a photo-cathode in the end wall of an r.f. cavity which supports a strong standing wave field. The advantages of this configuration are as follows:

- The electron bunch length is determined by the laser pulse length eliminating the need for a buncher and permitting narrow energy spread in the accelerated beam.
- Very low emittance beams can be produced by decreasing the laser spot size at the cathode.
- The r.f. cavity can support electric field gradients at the cathode of the order of 100MV/m which minimizes space-charge growth of the emittance when the electrons are nonrelativistic.
- A multicavity gun can deliver a beam of several MeV and can operate at the same frequency as the accelerator sections of the linac (2856MHz).

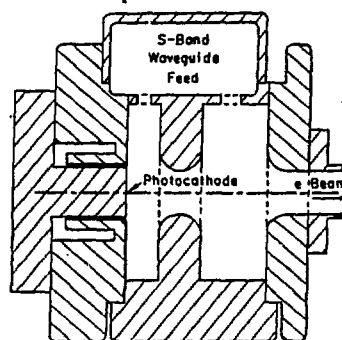


Figure 2. Section through the rf gun. Except for the waveguide feed the gun is axially symmetric. The 1 1/2-cells of the gun are 8 cm long.

Space charge fields are only important relative to the accelerating field strength at the cathode. With the high field proposed,  $\geq 100$  MV/m, only modest space charge growth will occur even for a relatively small bunch size. Once the electrons are relativistic space-charge emittance growth essentially ceases: thus all space-charge growth occurs within 1cm of the cathode surface. The field of the image of the bunch in the cathode plane serves to compress

MASTER

\*Work performed under the auspices of the U.S. Department of Energy

20

the bunch and actually reduces the space-charge growth by about 30%.

Thus the primary requirement for the r.f. gun is that the accelerating field at the cathode be large or an optimal cavity shape be chosen so that the r.f. fields cause minimal non-linear distortion of the phase of the bunch.

From a Fourier analysis of a standing wave field with circular symmetry we find there is an ideal form for which the transverse electric and magnetic fields have linear radial dependence. For the r.f. case it emerges that the length of a cell should be  $\lambda/2$  where  $\lambda$  is the wavelength of the r.f. field, and that the field in adjacent cells should be  $180^\circ$  out of phase i.e. operation should be in  $\pi$ -mode to minimize beam distortion. A  $\pi$ -mode configuration alone does not assure linear dependence of the transverse fields. However, a simple disc loaded structure utilizing thick discs and a large radius at the beam aperture provides a good enough approximation to the ideal so that r.f. induced emittance growth will be less than that due to space-charge.

The advantage of this configuration where, as shown in Figure 2, the cathode surface is at the mid-point of the first cell (i.e. the first cell is a half cell) is maximized if the electron bunch crosses the cell boundary when the electric fields vanish. Then the deflection of the beam as the bunch nears the aperture is cancelled by the opposite transverse fields encountered just beyond the entrance to the next cell. Thus the laser pulse should strike the photo-cathode at an r.f. phase somewhat less than  $90^\circ$  (where  $90^\circ$  corresponds to maximum electric field strength). Obviously there is no compensation at the exit of the last cell of the gun and in practice almost all of the r.f. induced emittance growth will occur there.

#### Photo-cathode Design

Ideally the photo-cathode should have picosecond response time, good quantum efficiency, good mechanical stability, low intrinsic emittance and long life time. For initial operation we will use a Yttrium metal cathode to emphasize reliability and later developments may include the use of a lower intrinsic emittance  $Cs_3Sb$  cathode.

The time response will be adequate if the photo electrons can cross an optical absorption length in less than a picosecond. An electron of 1eV can travel  $\approx 3000A_0$  in 1psec which is an order of magnitude greater than the absorption length of metals. Tests by members of the ATF Group (6) indicate a quantum efficiency for Yttrium metal illuminated by 4.65eV light (as for a frequency quadrupled Nd:YAG laser) is about  $2 \times 10^{-4}$ . The work function for Yttrium is about 3.1eV, so the photo electrons can emerge with up to 1.5eV. If the electrons are emitted with an isotropic regular distribution at the cathode surface this relatively high energy leads to an initial emittance of  $3.5 \times 10^{-6}$  m.rad. For a  $Cs_3Sb$  cathode the emittance would be about 1/3 of this value.

The cathode material will be deposited on a removable plug of 1cm radius in the end face of the gun. The plug will form one surface of an r.f. choke joint, which avoids the need for direct electrical contact between the plug and the nearby wall of the gun; the electron beam must, therefore, be deflected away from the laser optics shortly outside the gun. This arrangement also facilitates the use of a thermionic cathode for initial tests on the r.f. gun. Extremely good vacuum  $\approx 10^{-10}$  Torr is required in order to maintain the stability of the emitting surface.

#### R.F. Cavity Design

The program SUPERFISH<sup>7</sup> was used to calculate the resonant dimensions for the 1 1/2 cell gun cavity shown in Figure 2 but without the coupling waveguide connected so that the cavity maintained its circular symmetry. The resulting dimensions were then used as input data for the program MAFIA<sup>8</sup> which was used to calculate the change in the resonant frequency caused by the introduction of the coupling waveguide. If the coupling waveguide is operated in the standard  $TE_{10}$  mode it matches the way in which the magnetic field lines circulate in opposite senses in the two cells

of the electron gun for  $\pi$ -mode operation and essentially does not couple to the zero mode. In principle the coupling aperture can be adjusted together with a quarterwave short circuited waveguide termination, to exactly "match" the cavity to the waveguide. Because the programs SUPERFISH and MAFIA gave very different values for the resonant frequencies of the gun cavity (see Table II) we decided to build a brass model cavity to check resonant frequencies and coupling mechanisms.

TABLE II - Computed and Measured Resonant Frequencies for the 1 1/2 Cell Model of the Gun Cavity.

CONFIGURATION	RESONANT FREQUENCIES (MHZ)	
	ZERO MODE	$\pi$ -MODE
1 1/2 Cell Structure Without Waveguide Coupling System	2893.04	2894.95 (Superfish)
		2877.00 (Mafia)
1 1/2 Cell Structure with Waveguide Coupling System	2896.02	2897.88 (Measured)
		28171.02 (Mafia)
	2888.43	2890.30 (Measured)

Q value and field distribution measurements were made for several different cavity configurations as given in Table III. For each measurement the field was "flattened" or made equal at the cathode surface and the mid gap of the full cell, on axis, in the  $\pi$ -mode, by tuning the individual cells. It can be seen from Table III that the frequency of the  $\pi$ -mode was reduced by 7.28MMZ by introduction of the waveguide coupling system and the zero mode reduced by a similar amount. This coupling arrangement has a 1/2" wide slot extending over the full length of the gun cavity and the inner waveguide surface is tangential to the inner cylindrical surface of the cavity. With this configuration and with the waveguide short approximately one quarter guide wavelength beyond the slot center-line, the input VSWR was approximately 1.5. A quarter wave matching section was introduced into the waveguide just upstream of the coupling slot to improve the VSWR to better than 1.05.

TABLE III. SUMMARY OF RESONANT FREQUENCY AND Q-VALUE DATA FOR THE ELECTRON GUN TEST CAVITY

CAVITY CONFIGURATION	RESONANT FREQUENCY (MHZ)		MEASURED Q-VALUE	
	ZERO-MODE $\pi$ -MODE	ZERO-MODE $\pi$ -MODE	ZERO-MODE	$\pi$ -MODE
NO WAVEGUIDE, COUPLING VIA SMALL LOOPS; FIELD "FLAT" IN ZERO MODE	2896.02	2897.88	5523	5175
WAVEGUIDE CONNECTED AND TERMINATED AND COUPLED THROUGH 1/2" DIA. HOLES IN BOTH CELLS, MEASURED VIA SMALL LOOPS; FIELD "FLAT" IN $\pi$ -MODE (SHORT AT 24 cm.)	2892.92	2894.72	5350	4670
FINAL CONFIGURATION: WAVEGUIDE CONNECTED AND TERMINATED AND COUPLED THROUGH 1/2" WIDE SLOT COVERING BOTH CELLS. ALSO A 1/4" RADIUS HEMISPHERICAL HOLE CONNECTS THE TWO CELLS AT THE COUPLING SLOT. MEASURED VIA SMALL LOOPS; FIELD "FLAT" IN $\pi$ -MODE AND WAVEGUIDE SHORT AT 24 cm.	2888.45	2890.29	2490	2190
AS ABOVE BUT WITH WAVEGUIDE SHORT REDUCED TO 9.0 cm FROM SLOT CENTER	2888.43	2890.30	2600	2400
REPEAT MEASUREMENT AFTER REASSEMBLING AND RETUNING CAVITY	2877.72	2889.50	3700	2750

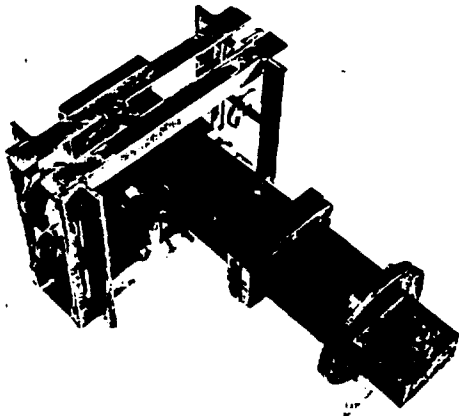


Figure 3. Model Cavity With Input Waveguide Connected.

With this final coupling configuration, which is shown in Figure 3, the Q values and resonant frequencies of the zero and  $\pi$ -modes were measured in two ways. First, the power was fed into the gun cavity via the waveguide feed system, and second the waveguide was terminated in a matched load and Q values measured in small coupling loops placed in the outer wall of each cell. The results are shown in Figure 4 from which it can be seen that when we feed through the waveguide the zero mode is essentially suppressed; whereas, when feeding through the small loops the zero mode is essentially unaffected by the waveguide coupling system, while the  $\pi$ -mode, which couples strongly to the loaded waveguide is reduced in Q value by approximately one half.

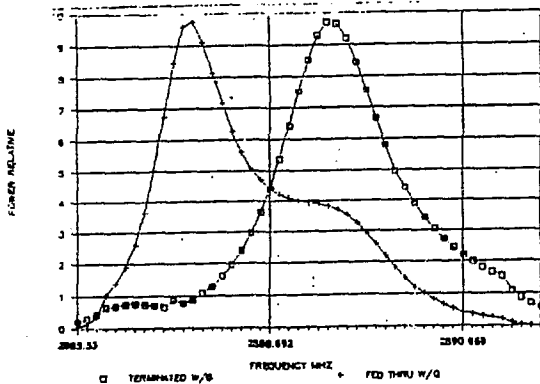


Figure 4. Final Q Plots with Waveguide Feed.

The axial electric field distribution was measured by the perturbation method and the effects of temperature and individual cell detuning on the axial field distribution were made. The electric field distribution across the diameter at a few different locations was also measured as follows:

- Adjacent to the cathode surface.
- Along the surface opposite the cathode surface in the short cell.
- Along the first surface of the large cell.
- Across the gap center of the large cell.

These results showed no asymmetry in the electric field distribution due to the coupling slot; a result which is confirmed by computations made with MAFIA.

#### Computer Simulations of Gun Performance

The emittance of the beam has been calculated with a version of the program PARMELA, modified to include ejection of low energy electrons from a photo-cathode by a laser pulse.

The photoelectrons are simulated with an energy spread of a fraction of an eV and with isotropic directions. They are emitted randomly with a profile that is gaussian in both radius and time, as for a laser pulse. The r.f. fields in the gun are taken from a Fourier analysis of a SUPERFISH calculation. The effect of Coulomb interactions among the electrons is calculated by a point-by-point code rather than the standard code of PARMELA, as the latter seemed less suitable for small bunches. The important effect of the image charges in the cathode plane is included. The simulation proceeds via a numerical integration of the equations of motion of the electron bunch, using the phase of the r.f. field as the time variable. We use the invariant emittance,  $\epsilon_x$ , defined below Table IV to characterize the transverse phase space.

Table IV.

Emittance Parameters	
Laser spot radius ( $\sigma$ in mm)	3
Laser pulse width ( $\sigma$ in psec)	2
Charge in bunch (n Coulomb)	1
$\epsilon_x^\dagger$ at cathode (mm-mrad)	3.5
$\Delta\epsilon_x$ due to self fields	6.2
$\Delta\epsilon_x$ due to rf fields	1.4
$\epsilon_x$ at exit	7.3
Beam energy spread ( $\sigma$ in keV)	17
Exit bunch length ( $\sigma$ in mm)	0.6
Exit bunch radius ( $\sigma$ in mm)	4.2
Exit beam angular divergence ( $\sigma$ in mrad)	28

$$\dagger \epsilon_x = \frac{1}{mc} \sqrt{\langle x^2 \rangle \langle x p_x^2 \rangle - \langle x p_x \rangle^2} = \sqrt{\langle x^2 \rangle \langle \gamma^2 \beta_x^2 \rangle - \langle x \gamma \beta_x \rangle^2}$$

The gun beam emittance parameters are given in Table IV. We use a cathode field of 100 MV/m, an initial electron energy of 1.5 eV and the electric field is a maximum at a phase of  $90^\circ$ . It can be seen from Table V that for the beam parameters given, there is an emittance growth,  $\Delta\epsilon_x$  of 6.2mm.mRad due to self fields and 1.4mm.mRad due to r.f. fields. These add roughly in quadrature to give an output emittance of 7.3mm.mRad. The output beam energy is 4.7 MeV and the energy spread,  $\sigma$ , is 17 KeV for an initial phase optimized at  $67^\circ$ . For this initial phase the electrons leave the gun almost exactly at a phase of  $360^\circ$ . The exit beam transverse phase space is shown in Figure 5 and the longitudinal in Figure 6.

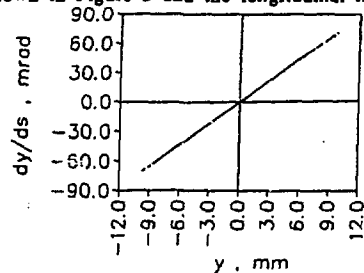


Figure 5. The transverse phase space at the exit of the rf gun for a bunch as given in the table.  $\sigma_x = 4.2$  mm,  $\sigma_x' = 28$  mrad, and  $\epsilon_x = 7.3$  mm-mrad.

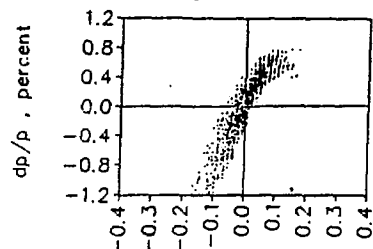


Figure 6. The longitudinal phase space at the exit of the gun.  $\sigma_z = 0.6$  mm, and  $\sigma_E = 17$  keV.

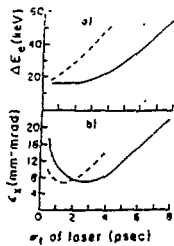


Figure 7. a) The beam energy spread  $\Delta E_e$ , and b) the transverse emittance  $\epsilon_x$  at the exit of the gun as a function of the laser pulse length. The solid (dashed) curves are for a peak rf field at the cathode of 100 (200) MV/m.

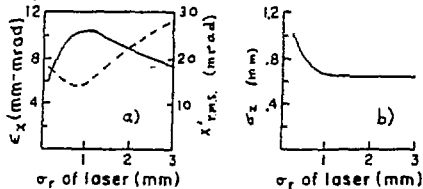


Figure 8. a) The transverse emittance  $\epsilon_x$ , (solid curve), and the r.m.s. beam divergence (dashed curve) as a function of the radius of the laser spot size on the cathode. b) The r.m.s. bunch length at the exit of the gun as a function of laser spot size. Other parameters are as in the table.

In Figure 7 we show the effect of varying the pulse length for peak cathode fields of 100MV/m and 200MV/m. It can be seen from Figure 7(b) that there is an optimum pulse length for the transverse emittance which results from the balancing of r.f. and self field effects. Figure 8 shows the dependency of  $\epsilon_x$  and the bunch length  $\sigma_z$  on the laser spot size. The r.m.s. divergence of the exit beam is also shown here.

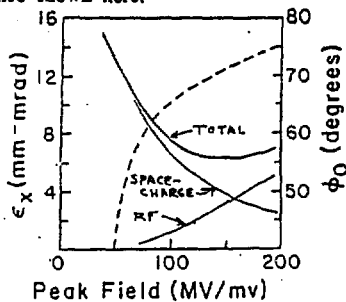


Figure 9. The transverse emittance (solid curves) as a function of the peak rf field on the cathode, and the optimum phase (dashed curve) for the laser pulse to strike the cathode. Other parameters are as in the table.

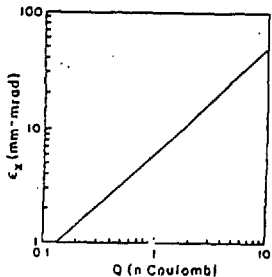


Figure 10. The transverse emittance  $\epsilon_x$  as a function of the charge of the electron bunch, with other parameters as in the table.

Figure 9 shows the effect of varying the peak field on the cathode and also the optimum r.f. phase for the laser pulse to strike the cathode to achieve the results shown. Finally in Figure 10 we show the emittance growth due to space charge alone as a function of total charge in the bunch. The trend is well described by  $\epsilon_x \sim Q^{0.9}$ . The beam brightness, which is proportional to  $Q/\epsilon_x \epsilon_y$ , varies with charge as  $Q^{-0.8}$  in the space charge limited region.

### Conclusion

The r.f. electron gun is clearly a strong candidate for the development of high brightness electron beams and when utilizing a laser driven photo-cathode should provide a very well defined electron beam for injection into conventional linac accelerating structure.

### Acknowledgment

The authors wish to thank R. Sheffield and L.M. Young of Los Alamos and R.H. Miller and W.B. Herrmannsfeldt of Stanford Linear Accelerator Center for many useful discussions and H. Ackerman, C. Biscardi and L. De Santo for their help with the model cavity measurements.

### References

- [1] R.B. Palmer, "A Laser-Driven Grating Linac," Part. Accel. vol. 11, pp. 81-90 (1980).
- [2] E. Courant et al., "Proposal for the Design and Construction of an IFEL Accelerator Demonstration Stage," BNL (1987).
- [3] R.C. Fernow et al., "Proposal for an Experimental Study of Nonlinear Thomson Scattering," Princeton University preprint DOE/ER/3072-39 (1986).
- [4] G.A. Loew, R.H. Miller and C.K. Sinclair, "The SLAC Low Emittance Accelerator Test Facility," 1986 Linear Accelerator Conference Proceedings, SLAC 303.
- [5] J.S. Fraser et al., "Photocathodes in Accelerator Applications," Proc. of the 1987 IEEE Particle Accelerator Conf., ed. by E.R. Lindstrom and L.S. Taylor (Washington, D.C., Mar. 16-19, 1987) pp. 1705-1709.
- [6] J. Fischer and T. Rao, private communication.
- [7] K. Halbach and R.F. Holsinger, Particle Accelerators 7 (1976) pp. 213.
- [8] R. Klatt et al., "MAFIA, A Three Dimensional Electromagnetic CAD System for Magnets, R.F. Structures and Transient Wake-Field Calculations," 1986 Linear Accelerator Conference Proceedings, SLAC 303.
- [9] K. Crandall, "PARMELA: A code for calculating Phase and Radial Motion in Electron Linear Accelerators," (Unpublished).